Frontiers in Heat and Mass Transfer

Tech Science Press

https://doi.org/10.32604/fhmt.2026.076292

ARTICLE

Modeling and Analysis on Flow Instability of Helical Coiled Tube Steam Generator of Liquid Metal Fast Reactor under Coupled Heat Transfer Conditions

Jialun Liu[1,2,3,*], Yuchang Lu[4], Jianjun Lin[3], Shebing Li[3], Ruixia Gao[5] and Zhao Li[6]

[1]College of New Energy, Xi'an Shiyou University, Xi'an, China
[2]School of Human Settlements and Civil Engineering, Xi'an Jiaotong University, Xi'an, China
[3]Longquan Zhongtai Auto Air Conditioner Co., Ltd., Lishui, China
[4]School of Mechanical Engineering, Xi'an Shiyou University, Xi'an, China
[5]School of Chemistry, Xi'an Jiaotong University, Xi'an, China
[6]College of Materials Science and Engineering, Xi'an Shiyou University, Xi'an, China

*Corresponding Author: Jialun Liu. Email: ljl.619@163.com

Received: 18 November 2025; Accepted: 03 February 2026; Published: 30 April 2026

ABSTRACT: A steady thermo-hydraulic model of the helical tube steam generator was first constructed to study the coupled heat transfer process between the primary and secondary sides based on a discrete modeling method, and obtain the heat flux density distribution along the steam generator. Then, taking the obtained coupled heat flux density distribution as the thermal boundary condition input, considering the dynamic variation of physical properties on the secondary side, a dynamic model based on the time-domain method suitable for two-phase flow instability among parallel multiple channels of the steam generator was constructed. Finally, taking the lead-bismuth fast reactor as an example, flow instability of the steam generator was analyzed under an inlet lead-bismuth temperature of 320°C~480°C and an inlet water temperature of 160°C~240°C. It was found that flow instability is less likely to occur under coupled heat conditions, compared with that under uniform or linear distribution. Flow excursion is prone to occur under low inlet temperature of the primary or secondary side. As the inlet lead bismuth temperature increases from 320°C to 480°C, average heat flux significantly increases by 2.5 times, and the non-uniformity of heat flux distribution increases of 49%. Meanwhile, the density wave oscillation amplitude gradually increases, and system stability weakens.

KEYWORDS: Liquid metal fast reactor; helical coiled tube steam generator; two-phase flow instability; discrete method; coupled heat transfer between primary side and second side

1 Introduction

As a typical representative of Generation IV reactors, liquid metal fast reactors have a relatively high outlet temperature of core coolant, and can achieve high thermoelectric conversion efficiency [1]. Helical coiled tube steam generator is widely used in various nuclear reactors, due to its advantages of compact structure, anti-expansion, and strong heat transfer performance [2]. Two-phase flow instability often occurs during the operation of steam generators, which includes static flow instability and dynamic flow instability. Static flow instability is known as flow excursion or Ledinegg instability. Dynamic flow instability includes pressure drop oscillation, thermal oscillation, and density wave oscillation. Among them, density wave oscillation is the most common and harmful. Flow instability phenomena always cause obvious oscillations of fluid pressure and flow rate, leading to mechanical oscillations and control problems [3]. Therefore,

studying and avoiding various types of flow instability has significant implications for the safe operation of steam generators.

Previous scholars have conducted relevant research on the flow instability of steam generators. Among them, most mathematicians conduct their research based on the assumed condition of uniform wall heating. For example, Peng et al. [4] used experiments and numerical simulations to study the flow excursion instability in parallel channels, pointing out that the decrease of gravity pressure drop in the hot channel caused by the increase of void fraction is the reason for the occurrence of flow excursion instability. Shen et al. [5] conducted experimental research about the influence of inlet subcooling on the flow instability in a parallel helical tube system under uniform heating conditions. Su et al. [6] established linear and nonlinear models and conducted numerical studies on three types of flow instabilities in the helical tube steam generator of High Temperature Gas-cooled Reactors (HTGR). Dong et al. [7] adopted RELAP5 program to study the flow instability in a two-channel parallel system with different tube types (helical tube and straight tube) under uniform heating conditions. Fu et al. [8] also used RELAP5 program to study the density wave flow instability in parallel vertical tubes under uniform heating conditions. Colombo et al. [9] conducted a numerical study on the density wave oscillation of two-phase flow in a single helical tube and parallel double helical tubes under uniform heating conditions by using RELAP5 program, and investigated the influence of structural parameters on the density wave oscillation. In addition, Liang et al. [10], Niu et al. [11], and Tang et al. [12] adopted the frequency domain method to study the flow instability in steam generators under uniform heating conditions.

Some scholars have also studied the flow instability phenomenon under non-uniform heating conditions by approximating and simplifying the heat transfer process. For example, Hou et al. [13] studied the density wave oscillation in parallel channels of a supercritical water-cooled reactor under different heat flux distribution patterns based on frequency domain modeling. They found that systems with a uniformly heat flux distribution are less stable than those with cosine-shaped or stair-shaped heat flux distributions. Liu et al. [14] approximately simulated the axial heat flux distribution under different powers in supercritical water-cooled reactors, calculated the stability boundary of parallel channel systems, and compared the results with those under uniform heating conditions. They found that the influence of axial heat flux distribution on system stability was not significant. Zhang et al. [15] used RELAP5 program to simulate the flow instability of a two parallel channel system under non-uniform heating conditions, assuming that the heat flux distribution follows a linear piecewise function. Liu et al. [16] studied the flow instability in parallel helical tubes under convective heating conditions by a one-dimensional program, and found that the system is more stable under convective heating conditions than under uniform heating conditions. Lu et al. [17] established a time-domain calculation model for density wave oscillation in a parallel channel system, assuming that the heat flux distribution approximately follows a cosine function, and studied the effect of non-uniform heat load distribution on flow instability. Wang et al. [18] built a 3×3 sub-channel model and simplified the heat flux distribution as a power curve consisting of two discontinuous linear segments. They studied the effects of the curve shape of the heat power distribution along the tube on the flow instability.

In the actual operation of the steam generator, heat exchange occurs between the working fluid in the secondary side and the working fluid in the primary side. During the flow and heat transfer process, the temperature and flow velocity of the working fluid on both sides constantly change, and the working fluid of the secondary side undergoes the phase transition process. This leads to an uneven distribution of heat load along the steam generator. Moreover, liquid metal fast reactors have a larger temperature difference along the primary side than that of pressurized water reactors [19,20], and the uneven distribution of heat load is significantly intensified. The existing research results based on the assumption of uniform or approximately

linear distribution of heat flux density are bound to be far from the actual operating conditions of steam generators in liquid metal fast reactors, resulting in limited guidance significance.

Therefore, the following two parts of the work were successively carried out in this paper. First, a steady thermo-hydraulic model of the helical tube steam generator is constructed to study the coupled heat transfer process between the primary and secondary sides based on a discrete modeling method, and obtain the heat flux density distribution along the steam generator. Second, taking the above coupled heat flux density distribution obtained by the steady thermo-hydraulic model as the thermal boundary condition input, considering the dynamic variation of physical properties on the secondary side, a dynamic model based on the time-domain method suitable for two-phase flow instability among parallel multiple channels of the steam generator was constructed. Finally, the two-phase flow instability in the helical coiled tube steam generator was calculated and analyzed under the coupled heat transfer conditions in the lead bismuth fast reactor.

2 Steady Thermal-Hydraulic Model

First, a steady thermal-hydraulic model was established to study the coupled heat transfer between two sides for the steam generator of a liquid metal fast reactor based on the discrete method. During the operation of the steam generator, the liquid metal of the primary side and water of the secondary side are arranged in countercurrent flow, and heat transfer occurs through the tube wall surface. Fig. 1 shows the basic structural schematic of the steady thermal hydraulic model.

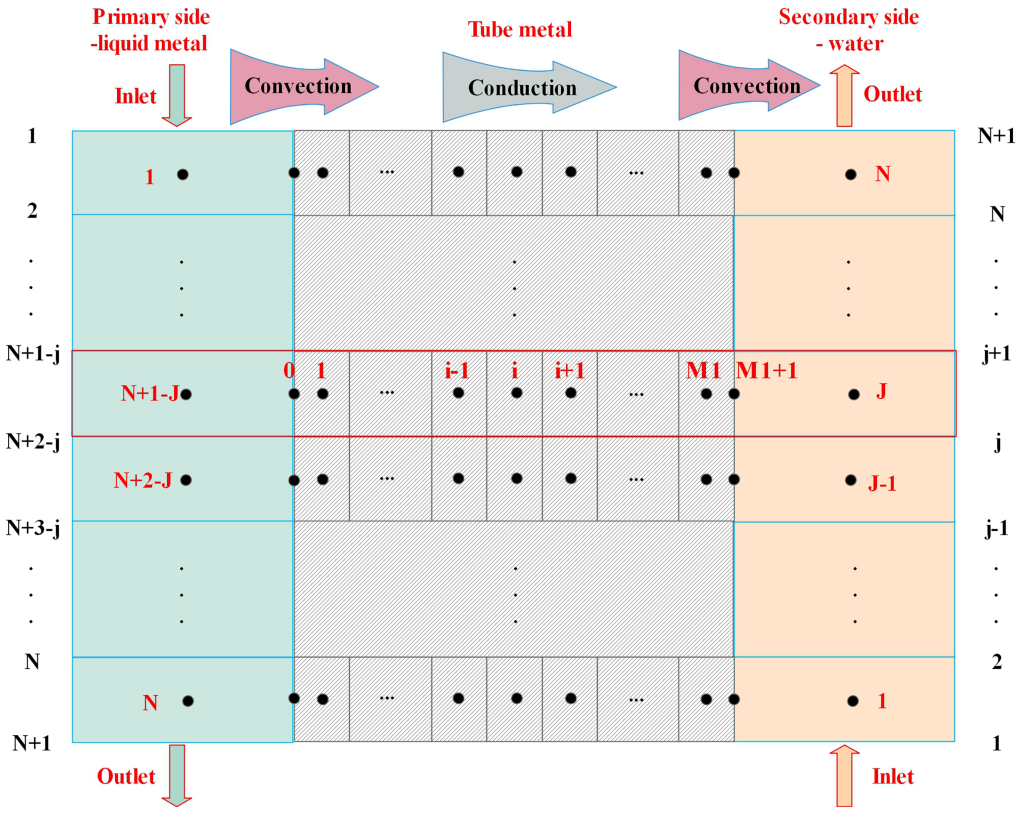

Figure 1: Structural schematic of the steady thermal-hydraulic model.

Fig. 1 indicates that the flow and heat transfer process of the entire steam generator can be divided into three regions, including the primary-side flow region, secondary-side flow region, and tube wall heat transfer region between two sides. The present model further divides the primary-side flow region and secondary-side flow region into grids along the flow direction, and also divides the tube wall into grids along the heat transfer direction. Then, the steady-state one-dimensional homogeneous N-S equations and the steady-state heat conduction equation are discretized for each grid of three regions by the finite difference method. Based on the steady thermal-hydraulic model, the distribution of parameters such as the temperature of the primary and secondary fluids, the wall temperature of the helical tube, and the heat flux can be calculated and obtained. More detailed introduction to the establishment and verification of the steady thermal-hydraulic model can be found in reference [21], which will not be repeated here.

3 Dynamic Two-Phase Instability Model

In this section, the time domain method was used to build a dynamic model to study the two-phase flow instability occur in the helical tube of the steam generator. Fig. 2 shows the schematic diagram of the parallel double helical tube system studied in this model.

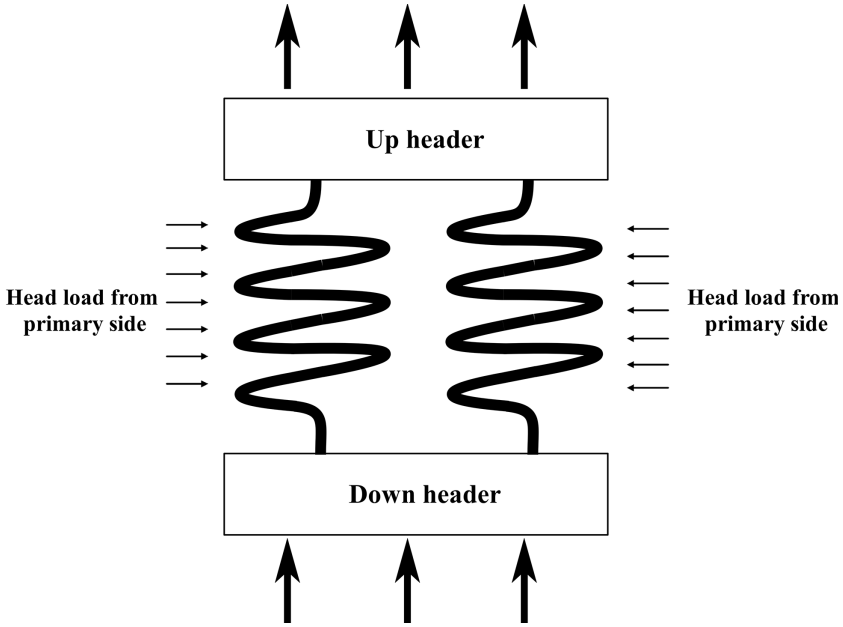

Figure 2: Schematic diagram of a parallel double helical tube system.

As shown in Fig. 2, two parallel helical tubes are connected between the upper and lower headers. The fluid flows into each tube from the lower header. During the upward flow along the tube, the fluid exchanges heat with the working fluid of the primary side outside the tube, undergoes phase changes, and finally flows out from the upper header.

The following one-dimensional homogeneous N-S partial differential equations are used to build the present models.

Conservation of mass equation:

$$A\frac{\partial \rho}{\partial t} + \frac{\partial M}{\partial z} = 0 \tag{1}$$

where M denotes fluid mass flow rate, A denotes cross-sectional area, and ρ denotes fluid density.

Momentum conservation equation

$$\frac{\partial M}{\partial t}+\frac{\partial}{\partial z}\left(\frac{M^2}{\rho A}\right)+A\frac{\partial P}{\partial z}+\frac{dP_{\mathrm{f}}}{dz}+\rho gA\sin(\theta)=0 \tag{2}$$

where P represents pressure; $\frac{dP_{\mathrm{f}}}{dz}$ is the frictional pressure drop gradient of fluid flowing along the channel; g is the gravity acceleration; θ is the helical rising angle.

Energy conservation equation:

$$A\frac{\partial(\rho h)}{\partial t}+\frac{\partial(Mh)}{\partial z}=Q_{\mathrm{l}} \tag{3}$$

where h denotes fluid enthalpy, and Q_{l} denotes heat load per unit length.

Besides, the following equations are also needed.

State equation:

$$\rho=f(P,h) \tag{4}$$

3.1 Discrete Equations

The working fluid inside the tube experiences a phase change caused by heating. In order to accurately consider the physical properties along the tube and the corresponding changes in resistance and heat transfer characteristics, the present model divides the flow region into a series of grids based on the discrete method and uses the finite difference method to solve the equations. Fig. 3 shows a schematic diagram of the mesh division along the flow region in any helical tube.

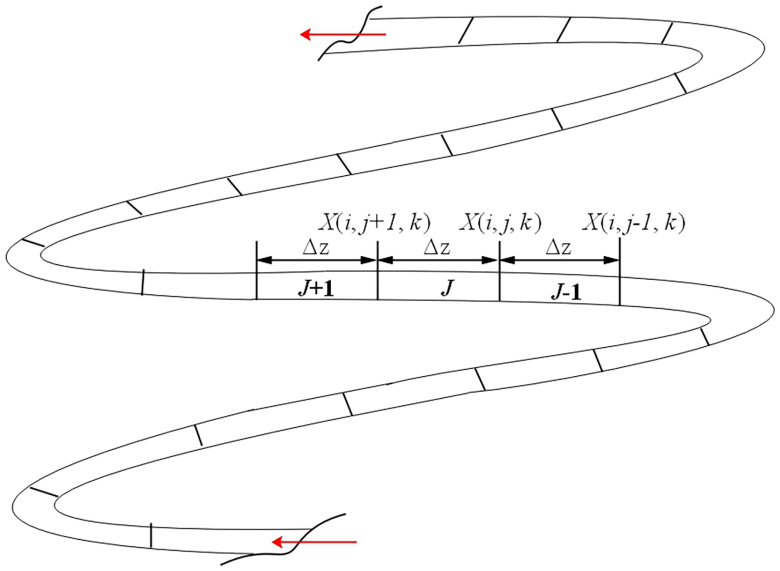

Figure 3: Mesh result of the flow region in the tube.

In Fig. 3, for any grid J along the tube i at time layer k, the inlet parameters are denoted by $X(i, j, k)$. Based on the above grid mesh method, the N-S partial differential Eqs. (1)–(3) are numerically discretized. For grid J, the discretized equations are expressed as Eqs. (5)–(7).

(1) Discretized mass conservation equation

$$\frac{A}{\Delta t}\left(\frac{\rho(i,j,k+1)+\rho(i,j-1,k+1)}{2}-\frac{\rho(i,j,k)+\rho(i,j-1,k)}{2}\right)+\frac{M(i,j,k+1)-M(i,j-1,k+1)}{\Delta z}=0 \tag{5}$$

(2) Discretized momentum conservation equation:

$$\frac{1}{\Delta t}\left(\frac{M(i,j,k+1)+M(i,j-1,k+1)}{2}-\frac{M(i,j,k)+M(i,j-1,k)}{2}\right)+\frac{1}{A\Delta z}\left[\left(\frac{M(i,j,k+1)^2}{\rho(i,j,k+1)}\right)-\left(\frac{M(i,j-1,k+1)^2}{\rho(i,j-1,k+1)}\right)\right]+A\frac{P(i,j,k+1)-P(i,j-1,k+1)}{\Delta z}+\frac{dP_f}{dz}\frac{\rho(i,j+1,k+1)+\rho(i,j,k+1)}{2}gA\sin\theta=0 \tag{6}$$

(3) Discretized energy conservation equation:

$$\frac{A}{\Delta t}\left(\frac{[\rho\cdot h](i,j,k+1)+[\rho\cdot h](i,j-1,k+1)}{2}-\frac{[\rho\cdot h](i,j,k)+[\rho\cdot h](i,j-1,k)}{2}\right)+\frac{[M\cdot h](i,j,k+1)-[M\cdot h](i,j-1,k+1)}{\Delta z}=Q(i,j,k+1) \tag{7}$$

3.2 Resistance Correlations

The fluid inside the helical tube undergoes three stages: subcooled water region, two-phase mixture region, and superheated steam region. The present model determines the state of the fluid in each grid by comparing the inlet fluid enthalpy with the corresponding enthalpy values of saturated water and steam.

For single-phase region, the frictional pressure drop gradient is calculated using the Ito formula [22].

$$\frac{dP_f}{dz}=f\frac{G^2}{2\rho d} \tag{8}$$

where G denotes mass flow rate, d denotes hydraulic diameter, and f is coefficient of frictional resistance. Under laminar flow conditions, the formula for calculating f is below [22].

$$f=f_s\cdot 21.5\cdot \mathrm{De}/\left(1.56+\log_{10}\mathrm{De}\right)^{5.73} \tag{9}$$

where f_s is the corresponding straight tube resistance coefficient, De is the Dean number, which is calculated by the following equation.

$$\mathrm{De}=\mathrm{Re}\sqrt{\frac{d}{D_c}} \tag{10}$$

where Re denotes Reynolds number, and D_c denotes helical diameter.

Under turbulent conditions, the formula for calculating f is below [22]:

$$f=0.304\mathrm{Re}^{-0.25}+0.029\left(d/D_c\right)^{0.5} \tag{11}$$

For two-phase flow, frictional pressure drop gradient is calculated by the formula proposed by Santini et al. [23].

$$\frac{dP_f}{dz} = \left(-0.0373x^3 + 0.0387x^2 - 0.00479x + 0.0108\right)\frac{G^{1.91}}{\rho \cdot d^{1.2}} \tag{12}$$

where x is the steam quality.

3.3 Boundary Conditions

Boundary conditions are set as below:

(1) The total inlet mass flow rate of the system is known.
(2) The inlet fluid enthalpy of the system is known.
(3) The inlet fluid pressure of the system is known.
(4) The outlet pressure of each tube is equal.
(5) The heat load along the tube wall is known.

In the above boundary condition (5), the heat flux density distribution is obtained from the coupled heat transfer process between two sides of the steam generator, and it can be calculated by the steady thermal hydraulic model in Section 2 of this paper.

3.4 Model Verification

(1) Verification for density wave instability

Wang et al. [24] conducted an experiment to study two-phase flow instability in two parallel helical tubes, and obtained the threshold heat power values for density wave instabilities that occurred under different inlet fluid quality (x_{in}). The related structural parameters and operation parameters are shown in Table 1.

Table 1: Parameters set in verification examples.

Parameters	Values
Tube length	4.79 m
Tube diameter	9 mm
Helical diameter	0.35 m
Helical angle	10°
Local resistance coefficient	45
Inlet water pressure	2.0 MPa

Fig. 4 shows the calculated results of the model in this work, as well as the corresponding experimental values.

Fig. 4 shows that the calculated values show good agreement with the experimental values, and the relative deviation of the predicted results from the experimental data shall not exceed 4% within the operating range of the examples.

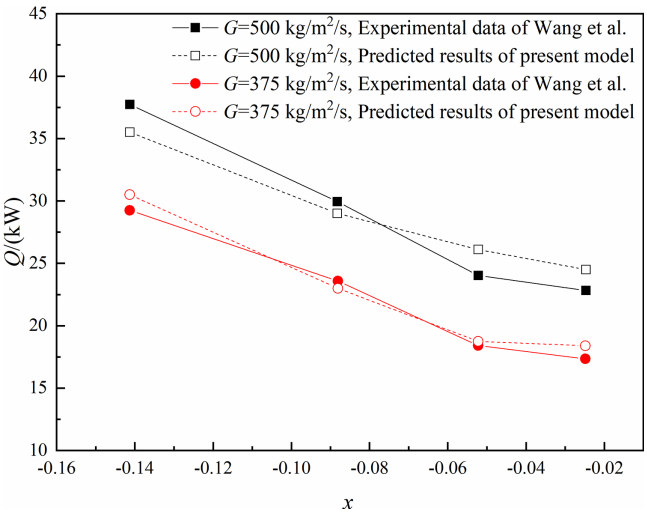

Figure 4: The verification for density wave instability.

(2) Verification for flow excursion instability

Papini et al. [25] conducted an experimental study on two-phase instabilities in the parallel helically coiled channels of a steam generator, and the experimental data were used to verify the reliability of the prediction for flow excursion by the present model. In their experiment system, the test section consists of two channels, each with a length of 32 m. The first 24 m of the channel is heated, while the remaining 8 m is unheated. The flow rates in the two channels were recorded in the presence of a flow excursion instability (system parameters: P = 24 bar, Tin = 134°C, Q = 46.5 kW). Fig. 5 shows the comparison of the predicted results by the present model with the experimental data.

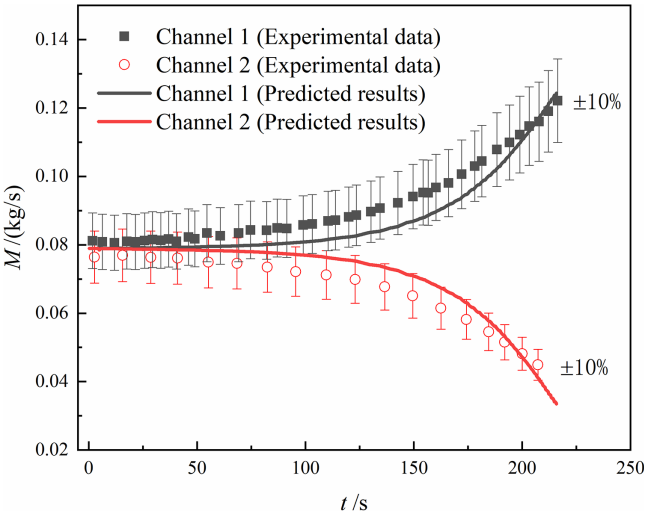

Figure 5: The verification for flow excursion instability.

In Fig. 5, it can be found that the predicted results show a good agreement with the experimental data, and the flow rates of the two channels gradually diverge from each other, exhibiting an obvious flow excursion phenomenon under the current operating conditions.

4 Results and Discussions

In this section, the flow instability in two parallel helical tubes is investigated under coupled heat transfer conditions. Based on the actual conditions of a lead bismuth fast reactor, multiple sets of examples are designed to calculate the heat flux distribution, thermodynamic equilibrium quality distribution, and flow rate oscillation curves in the steam generator at different inlet lead bismuth temperatures of 320–480°C and different inlet water temperatures of 160–240°C. In the calculation, the length and diameter of the tube are 20 m and 500 mm, respectively; the inner diameter of the tube is 9 mm, and the helical angle is 6°. The inlet fluid pressure and inlet fluid mass flow rate of the secondary side are 5.0 MPa and 1000 kg/(m^2·s), respectively, while the lead bismuth velocity is 0.5 m/s. To focus on investigating the occurrence characteristics of flow instability phenomena, this study specifically designs a series of low-load operating conditions where the secondary side outlet is saturated steam.

Before conducting computational analysis, it is necessary to verify the independence of the time step and spatial step set in the model. Fig. 6 shows the calculation results of the threshold heat load (Q_c) of the parallel helical tube system at different time steps and spatial steps, respectively.

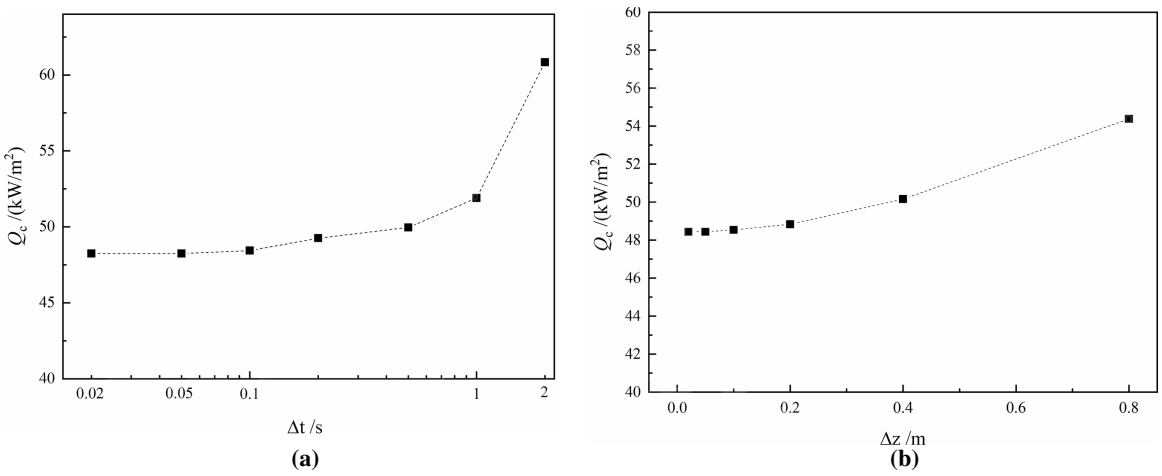

Figure 6: Grid independence verification results: (**a**) Time step independence verification; (**b**) Spatial step independence verification.

Fig. 6a indicates that when the time step is less than 0.05 s, the threshold heat load value almost no longer changes with the decrease of time step. Therefore, the time step is set as 0.05 s in this model. Meanwhile, Fig. 6b indicates that when the spatial step size is less than 0.05 m, the threshold heat load value almost no longer changes with the decrease of spatial step. Therefore, the spatial step is set as 0.05 m in this model.

4.1 Influence of Heat Load Distribution

In this section, the heat load distribution along the tube under the coupled heat transfer conditions is first calculated by the steady thermal-hydraulic model, as shown in Fig. 7. In the calculation, the inlet temperature of lead bismuth on primary side ($T_{lb,in}$) is 400°C, and inlet temperature of water on secondary side ($T_{f,in}$) is 200°C. In addition, existing related research often simplifies the heat load distribution into a uniform distribution or a linear distribution. In order to study the influence of heat load distribution, Fig. 7 also presents four different linear heat flux distributions with different slopes (K = 0, 0.5, 1.0, 2.0), and the

uniform heat flux distribution can be considered as a linear distribution with slope K = 0. The average heat flux (Q_{avg}) remains constant under all heat flux distribution patterns.

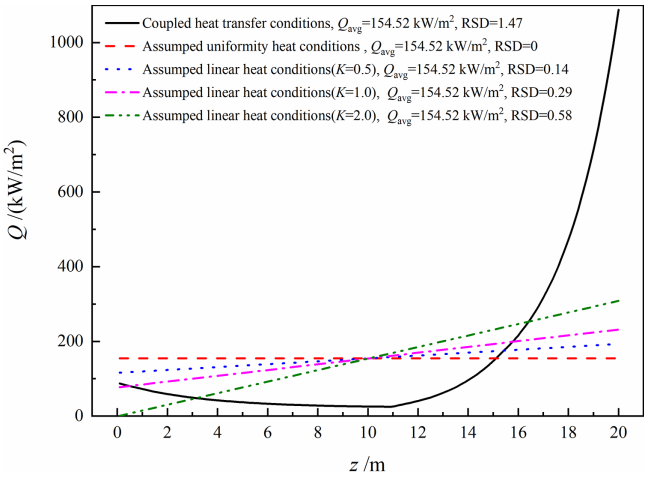

Figure 7: Heat load distribution results under different heat boundary conditions.

In Fig. 7, it can be seen that under the coupled heat transfer conditions, the heat load distribution is extremely non-uniform along the tube. Firstly, the fluid at the front of the tube section is in a single-phase subcooled water state, and heat transfer coefficients on the inner wall surface are generally low, resulting in a relatively low heat flux density. As the fluid continues to be heated along the flow direction, the temperature difference between water and lead bismuth gradually decreases, resulting in a gradual decrease in heat flux density. At the position of z = 10.9 m, the fluid inside the tube reaches saturation temperature and begins to enter the nucleate boiling region. The inner wall heat transfer coefficient sharply increases, resulting in a sudden increase in heat flux density between two sides. At the outlet of the tube section, the heat flux density reaches its peak. The maximum and minimum values of heat flux density are about 1087.4 and 25.1 kW/m^2, and there exists a difference of 43 times between them. The relative standard deviation (RSD) is adopted to characterize the uniformity of heat flux density distribution along the tube, and the calculation method is as follows.

$$RSD = \frac{\sqrt{\frac{\sum_{j=1}^{N}\left(Q(j)-\overline{Q}\right)^2}{N-1}}}{\overline{Q}} \tag{13}$$

where $\overline{Q}$ is the average value of the heat flux corresponding to all grids along the tube.

According to the calculation, the RSD of the heat flux distribution under coupled heat transfer conditions is 1.47, which is much higher than the corresponding values under uniform heat flux distribution and linear heat flux distribution conditions.

Fig. 8 indicates the oscillation curve of inlet mass flow rate in parallel helical tubes calculated under different heat flux boundary conditions, as defined in Fig. 7, calculated by the dynamic instability model.

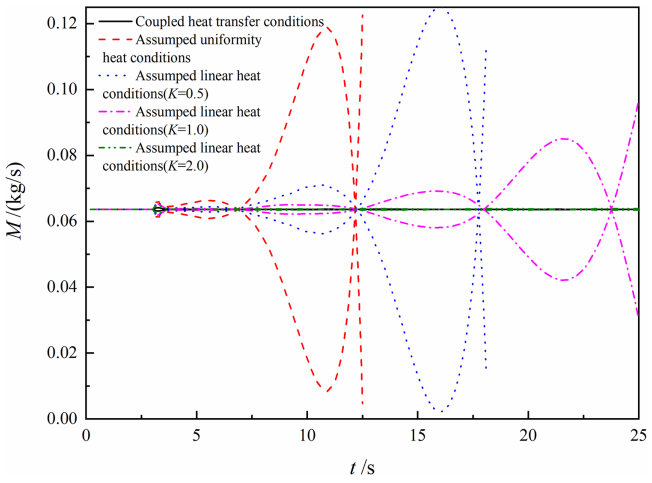

Figure 8: Calculation results of inlet mass flow oscillation curves under different heat boundary conditions.

Fig. 8 declares that the oscillation curve of mass flow rate tends to converge, and the system quickly returns to stability under the coupled heat transfer conditions. Under the condition of linear heat flux distribution, the oscillation curve of mass flow rate in the tube shows a significant divergence trend. As the distribution slope K increases, the divergence trend of the oscillation curve slows down significantly, and the system stability is enhanced. Under the condition of uniform heat flux distribution (K = 0), the divergence trend of the oscillation curve is the most severe, the oscillation amplitude rapidly expands, and the system is the most unstable. The main reason can be explained below. The heat flux density in a long tube section from the tube inlet (0 m < z < 15 m) under the coupled heat transfer conditions is further lower than that under the condition of linear heat flux distribution. This directly leads to a significantly longer length of the single-phase subcooled water section and a relatively shorter length of the two-phase evaporation section inside the tube. Fig. 9 shows the fluid quality distribution (x) along the helical tube under different heat boundary conditions. The length of subcooled water section (L_s) and the length of two-phase evaporation section (L_t) inside the tube under different heat boundary conditions are also shown in Fig. 9.

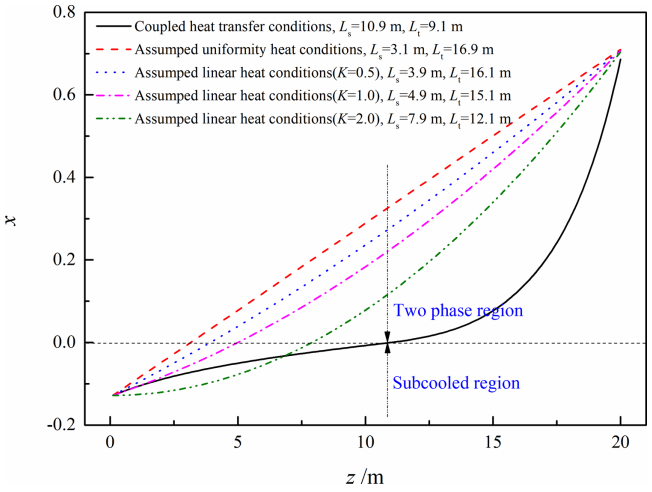

Figure 9: Fluid quality distribution results under different heat boundary conditions.

It can be clearly seen from Fig. 9 that under the coupled heat transfer conditions, the length of subcooled water region (L_s) is 10.9 m, and the length of the two-phase evaporation section (L_t) is only 9.1 m. Under the condition of uniform heat flux distribution, the corresponding length of the single-phase subcooled water region is 3.1 m, which is only one-third of L_s under the coupled heat transfer conditions. Meanwhile, as the slope K of the linear distribution increases, L_s also increases and L_t gradually decreases. The main reason for this is that as the slope K increases, the wall heat flux density of the front section of the tube near the inlet gradually decreases, which means the inlet working fluid needs to flow through a longer distance to be heated to saturation temperature. In general, the compressibility of the liquid in the subcooled water region is very weak, which can hinder the oscillation of the flow rate inside the tube. In the two-phase region, the working fluid undergoes a phase transition, resulting in significant density changes and promoting the occurrence of density wave oscillation. The larger the ratio of L_s to L_t, the more stable the system becomes [26]. Therefore, as the slope K of the linear distribution increases, the density wave oscillation trend weakens and the system stability enhances.

4.2 Influence of Inlet Lead Bismuth Temperature in Primary Side

Fig. 10 declares the heat load distribution of the inner tube wall at different inlet lead bismuth temperatures ($T_{lb,in}$ = 320°C~480°C) calculated by the steady thermal-hydraulic model. Among them, the inlet water temperature in secondary side is 160°C.

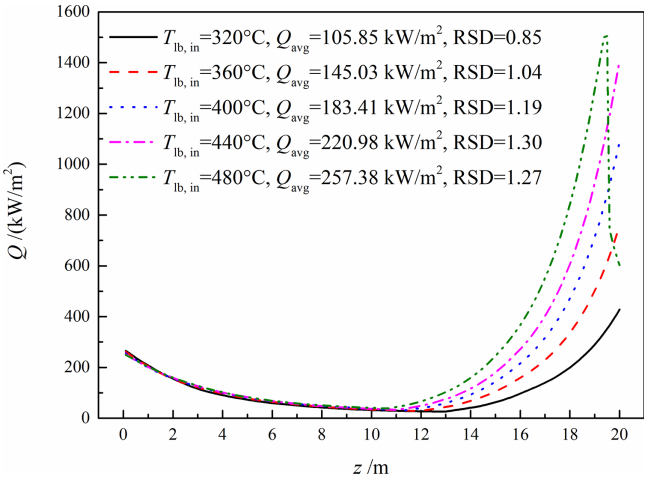

Figure 10: Heat load distribution results under different inlet lead bismuth temperatures of 320°C~480°C.

Fig. 10 shows that the heat load between two sides gradually increases with the increase of $T_{lb,in}$, especially in the section near the outlet of the helical tube, where the heat flux density increases significantly. As $T_{lb,in}$ gradually increases from 320°C to 480°C, the average heat flux density (Q_{avg}) along the steam generator gradually increased from 105.85 to 257.38 kW/m^2, with an increase of approximately 2.5 times. The peak heat flux density increased from 427.82 to 1515.86 kW/m^2, increasing by nearly 3.5 times. The main reason for this can be explained below. As the inlet lead bismuth temperature increases, the temperature difference between the two fluids gradually increases. Moreover, the increase in heat transfer temperature difference is more significant in the section near the outlet of the helical tube, due to the counter flow arrangement of the steam generator. This leads to an increase in heat transfer between the two sides. Fig. 10 also indicates that as $T_{lb,in}$ gradually increases from 320°C to 480°C, the relative standard deviation (RSD) of the heat flux distribution along the steam generator shows a gradually increasing trend from 0.85 to 1.27,

increasing by 49%. This indicates that the heat flux density distribution gradually becomes more uneven. At $T_{lb,in}$ = 480°C, the maximum value and minimum value of heat flux density are 1515.86 and 39.07 kW/m^2, and the difference between them is approximately 40 times. Fig. 11 represents the fluid quality distribution results along the helical tube under different inlet lead bismuth temperatures ranging from 320°C to 480°C.

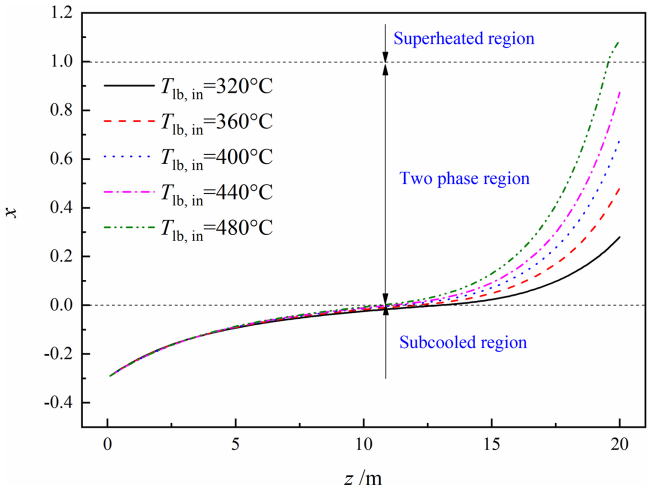

Figure 11: Fluid quality distribution result under different inlet lead bismuth temperatures of 320°C~480°C.

In Fig. 11, it can be seen that as $T_{lb,in}$ increases, the heat load between two sides gradually increases, and the fluid quality at the outlet of the secondary side gradually increases. Especially in the two-phase region, the variation in fluid quality along the tube becomes more pronounced as $T_{lb,in}$ increases. When $T_{lb,in}$ increases to 480°C, the fluid at the outlet has reached a superheated steam state, with a thermal equilibrium quality of nearly 1.1. Fig. 12 further shows the oscillation curves of the inlet mass flow rate in two parallel helical tubes under different inlet lead bismuth temperatures of 320°C~480°C calculated by the dynamic instability model.

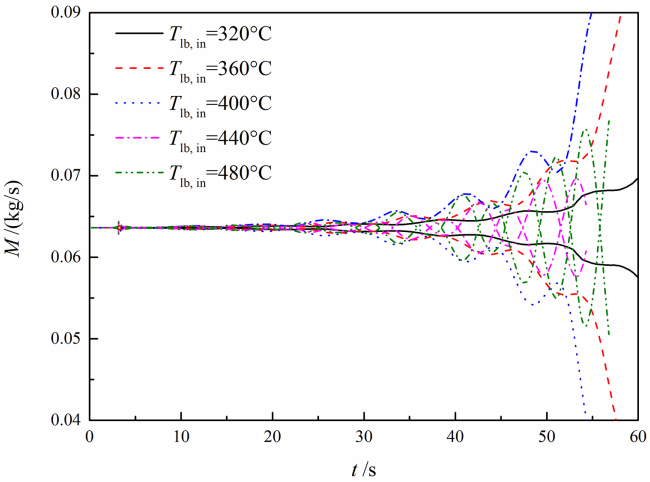

Figure 12: Calculation results of inlet mass flow oscillation curves under different inlet lead bismuth temperatures of 320°C~480°C.

Fig. 12 indicates that the inlet mass flow rate in parallel helical tubes exhibits two typical flow instability phenomena at different inlet lead bismuth temperatures. Firstly, under the condition of relatively low inlet

lead bismuth temperature ($T_{lb,in}$ = 320°C~400°C), the flow excursion instability occurs in the inlet mass flow rate of two tubes. The flow rate of the working fluid in the tube gradually deviates from the initial steady-state value, accompanied by the appearance of out-of-phase density wave oscillation. As $T_{lb,in}$ increases, the phenomenon of flow excursion intensifies, and the mass flow rate of the two tubes rapidly deviates from the steady-state value, indicating that the system becomes more unstable. When $T_{lb,in}$ increases to 440°C, the flow excursion phenomenon disappears, and the inlet mass flow rate of the two tubes shows single out-phase density wave oscillation and tends to diverge. As $T_{lb,in}$ continues to increase, the oscillation amplitude of mass flow rate also increases, the divergence trend becomes more obvious, and the system stability is significantly weakened. The above law of two typical flow instability phenomena is related to the variation curve of pressure drop with flow rate of the parallel helical tube system in the secondary side ("ΔP–G curve"). The flow excursion instability generally occurs in the negative slope region of ΔP–G curve [27]. Fig. 13 shows the corresponding ΔP–G curve under different inlet lead bismuth temperatures ($T_{lb,in}$ = 320°C~480°C). In the calculation of the above examples in Fig. 12, the mass flow rate of the parallel helical tube system is 1000 kg/(m^2·s).

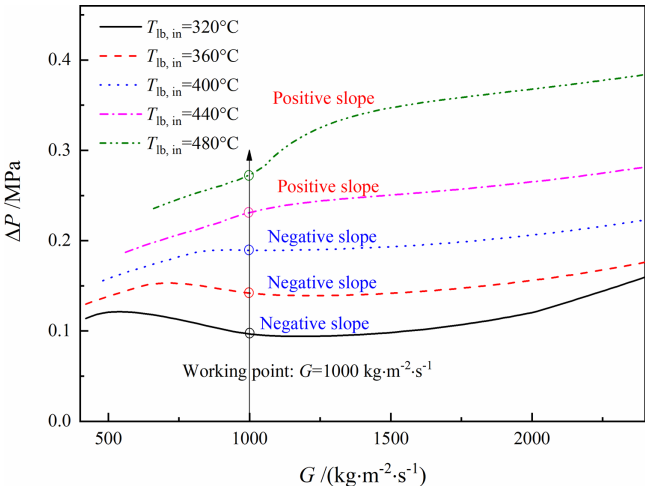

Figure 13: Calculation results of ΔP–G curve under different inlet lead bismuth temperatures of 320°C~480°C.

Fig. 13 indicates that the working conditions in the tube are all located in the negative slope region of ΔP–G curve under the conditions of low inlet lead bismuth temperature ($T_{lb,in}$ = 320°C~400°C), resulting in the occurrence of the flow excursion phenomenon. Under these conditions of $T_{lb,in}$ = 320°C~400°C, the heat load values along the tube are relatively small, and the steam quality at the outlet is low. Therefore, the fluid density variation along the helical tube is relatively weak, the amplitude of density wave oscillation is also relatively weak. As $T_{lb,in}$ increases ($T_{lb,in}$ = 440°C~480°C), the wall heat flux density gradually increases, and the steam quality at the outlet of the secondary side gradually increases, even reaching the superheated steam state. At this time, the working condition in the tube is located in the positive slope region of ΔP–G curve, and the flow excursion phenomenon disappears. However, the density changes experienced by the fluid are significantly intensified under higher $T_{lb,in}$ of 440°C~480°C, so stronger density wave oscillation between the tubes is induced.

4.3 Effects of Inlet Water Temperature in Secondary Side

Fig. 14 indicates the heat load distribution at different inlet water temperatures in the secondary side ($T_{f,in}$ = 160°C~240°C) calculated by the steady thermal-hydraulic model. Among them, $T_{lb,in}$ is 400°C.

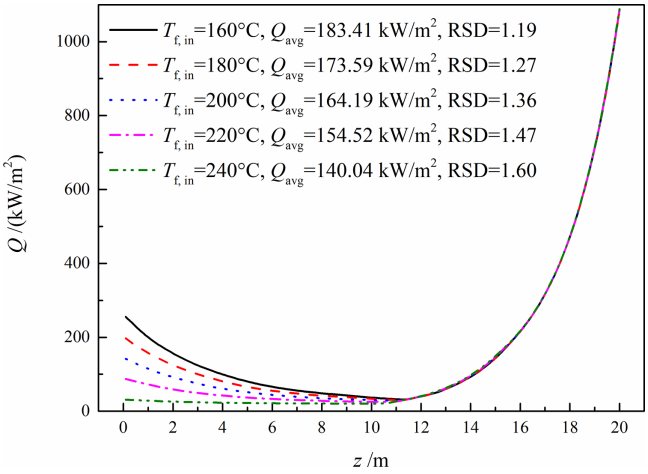

Figure 14: Heat load distribution result under different inlet water temperatures of 160°C~240°C.

Fig. 14 indicates that as $T_{f,in}$ increases, the temperature difference between water and lead bismuth is bound to decrease, resulting in a weakened heat exchange between two sides. The average heat flux density (Q_{avg}) gradually decreases from 183.41 to 140.04 kW/m^2, decreasing by about 24%. Fig. 14 also declares that as $T_{f,in}$ gradually increases from 160°C to 240°C, the relative standard deviation of heat load distribution along the steam generator (*RSD*) increases from 1.19 to 1.60, increasing by 34%. This indicates that heat load distribution gradually becomes more uneven. Besides, it should be noted that there is almost no difference in the outlet fluid temperature under different inlet water temperatures of 160°C~240°C. Fig. 15 further illustrates the fluid quality distribution (x) of the secondary side along the helical tube under different inlet water temperatures ($T_{f,in}$ = 160°C~240°C).

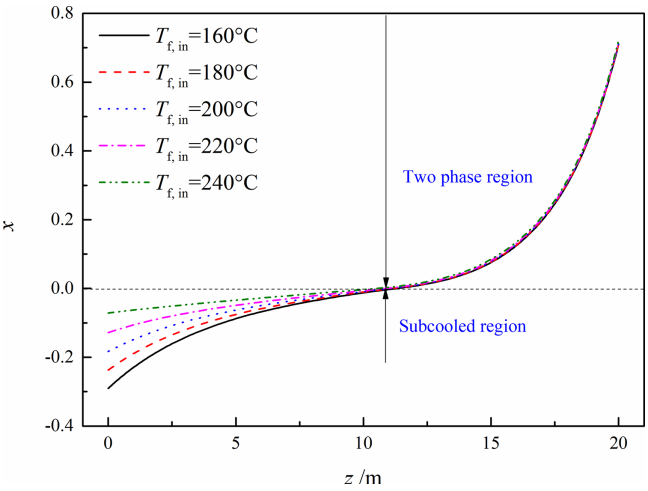

Figure 15: Fluid quality distribution result under different inlet water temperatures of 160°C~240°C.

Fig. 15 indicates that there is almost no obvious change in the fluid quality at the outlet, due to the constant $T_{lb,in}$. When the inlet water temperature is low, the wall heat flux density near the inlet of the tube is also high, caused by a higher heat transfer temperature difference, and the fluid quality also changes more dramatically. Fig. 16 further shows the oscillation curves of the inlet mass flow rate in two parallel helical

tubes under different inlet water temperatures of the secondary side ($T_{f,in}$ = 160°C~240°C) calculated by the dynamic instability model.

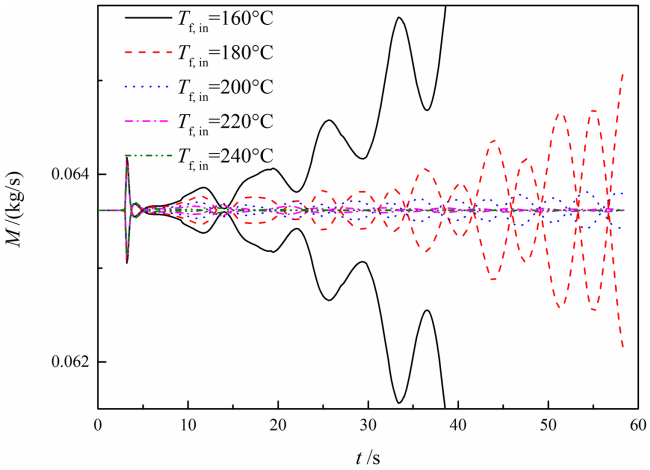

Figure 16: Calculation results of inlet mass flow oscillation curves under different inlet water temperatures of 160°C~240°C.

Fig. 16 declares that when $T_{f,in}$ is 160°C, there is a significant flow excursion phenomenon, accompanied by divergent density wave oscillation characteristics, resulting in a rapid deviation of the mass flow rate from the steady-state value. When the inlet water temperature increases to 180°C, the phenomenon of flow excursion disappears, and the flow rate between two tubes exhibits divergent out-of-phase density wave oscillation. As the inlet water temperature continues to increase, the oscillation trend of the mass flow rate between two tubes tends to converge, the amplitude gradually weakens, and the system stability is enhanced. When the inlet water temperature increases to 240°C, the oscillation trend of the flow rate is already very weak, and quickly recovers to the initial steady-state value.

5 Conclusions

In this paper, a steady thermal-hydraulic model was first established to study the coupled heat transfer between two sides of the helical tube steam generator in liquid metal fast reactors, and then a dynamic model was established to study the two-phase flow instability among parallel multiple channels under coupled heat transfer conditions. According to the lead bismuth fast reactor, the flow instability between two parallel helical tubes was calculated and analyzed within the operating conditions of inlet lead bismuth temperature of 320°C~480°C and inlet water temperature of 160°C~240°C. The following conclusions are obtained.

(1) The heat flux distribution between two sides of steam generator is extremely uneven, showing a trend of slowly decreasing from the inlet and then sharply increasing near the outlet. Under the coupled heat transfer condition, the flow instability is less likely to occur, and the system stability is stronger, compared to uniform heat flux distribution or linear heat flux distribution.

(2) Flow excursion instability is prone to occur under the conditions of low inlet lead bismuth temperature, and density wave instability also occurs simultaneously. As the inlet lead bismuth temperature increases, the phenomenon of flow excursion gradually disappears, the amplitude of density wave oscillation gradually increases, and the system stability weakens.

(3) Similarly, flow excursion instability is prone to occur under the conditions of low inlet water temperature, and density wave instability also occurs simultaneously. As the inlet water temperature increases,

the phenomenon of flow excursion gradually disappears, the amplitude of density wave oscillation gradually decreases, and the system stability enhances.

Acknowledgement: Not applicable.

Funding Statement: This work is supported by Natural Science Basic Research Program of Shaanxi Province (Grant Nos. 2025JC-YBMS-475, 2025JC-YBMS-420), Joint Funds of the National Natural Science Foundation of China (Grant No. U20B2036), and National Natural Science Foundation of China (Grant No. 52274064).

Author Contributions: The authors confirm contribution to the paper as follows: conceptualization, Jialun Liu; software, Jialun Liu; validation, Yuchang Lu, Zhao Li; investigation, Yuchang Lu; resources, Shebing Li; data curation, Yuchang Lu; writing—original draft preparation, Jialun Liu; writing—review and editing, Ruixia Gao; supervision, Ruixia Gao; project administration, Jianjun Lin. All authors reviewed and approved the final version of the manuscript.

Availability of Data and Materials: The authors confirm that the data supporting the findings of this study are available within the article.

Ethics Approval: Not applicable.

Conflicts of Interest: The authors declare no conflicts of interest.

References

1. Liu Y, Duan D, Deng C, Zhu Y, Wang Y, Zhang Y, et al. Experimental study on fluid-structure interaction of multiple support barrels in liquid metal fast reactor. Prog Nucl Energy. 2024;171:105163. doi:10.1016/j.pnucene.2024.105163.
2. Caramello M, Bertani C, De Salve M, Panella B. Helical coil thermal-hydraulic model for supercritical lead cooled fast reactor steam generators. Appl Therm Eng. 2016;101(1):693–8. doi:10.1016/j.applthermaleng.2016.01.028.
3. Li C, Fang X, Dai Q. Two-phase flow boiling instabilities: a review. Ann Nucl Energy. 2022;173(74):109099. doi:10.1016/j.anucene.2022.109099.
4. Peng CX, Zan YF, Yuan DW, Zhuo WB, Xu JJ, Huang YP. Research on hydrodynamic drift instability of parallel channels. Nucl Power Eng. 2021;42(S1):17–20. (In Chinese). doi:10.13832/j.jnpe.2021.S1.0017.
5. Shen C, Liu M, Xu Z, Cheng K, Liu L, Gu H. Study on two-phase flow instability of parallel helical tubes in steam generator of small modular reactors. Int Commun Heat Mass Transf. 2023;148(10):107023. doi:10.1016/j.icheatmasstransfer.2023.107023.
6. Su Y, Li X, Wu X. Two-phase flow instability characteristics of HTGR once through steam generators. Nucl Eng Des. 2023;415:112697. doi:10.1016/j.nucengdes.2023.112697.
7. Dong R, Niu F, Zhou Y, Yu Y, Guo Z. Modeling analyses of two-phase flow instabilities for straight and helical tubes in nuclear power plants. Nucl Eng Des. 2016;307(10):205–17. doi:10.1016/j.nucengdes.2016.07.001.
8. Fu W, Li XW, Wu XX, Zhang ZM. Investigation on two-phase flow density wave instability in parallel once-through evaporation tubes. J Eng Thermophys. 2014;35(3):576–80. (In Chinese).
9. Colombo M, Cammi A, Papini D, Ricotti ME. RELAP5/MOD3.3 study on density wave instabilities in single channel and two parallel channels. Prog Nucl Energy. 2012;56(1):15–23. doi:10.1016/j.pnucene.2011.12.002.
10. Liang Q, Li X, Su Y, Wu X. Frequency domain analysis of two-phase flow instabilities in a helical tube once through steam generator for HTGR. Appl Therm Eng. 2020;168:114839. doi:10.1016/j.applthermaleng.2019.114839.
11. Niu F, Tian L, Yu Y, Li R, Norman TL. Studies on flow instability of helical tube steam generator with Nyquist criterion. Nucl Eng Des. 2014;266:63–9. doi:10.1016/j.nucengdes.2013.10.026.
12. Tang Y, Zhou Z, Zhang D. Investigation of density wave instability in once-through superheated steam generators using SIGHT. Ann Nucl Energy. 2017;109(1):41–51. doi:10.1016/j.anucene.2017.05.027.
13. Hou D, Lin M, Liu P, Yang Y. Stability analysis of parallel-channel systems with forced flows under supercritical pressure. Ann Nucl Energy. 2011;38(11):2386–96. doi:10.1016/j.anucene.2011.07.021.

14. Liu P, Hou D, Lin M, Kuang B, Yang Y. Stability analysis of parallel-channel systems under supercritical pressure with heat exchanging. Ann Nucl Energy. 2014;69(2):267–77. doi:10.1016/j.anucene.2014.02.021.
15. Zhang W, Zhang TQ, Shi HL, Wang C, Li JS. Simulation of flow instability in parallel two channels under non-uniform heating and asymmetric heating conditions. At Energy Sci Technol. 2022;56(S1):42–9. (In Chinese). doi:10.1016/j.anucene.2013.07.030.
16. Liu M, Shen C, Xu Z, Zeng C, Wang X, Liu L, et al. Numerical study on flow instability of parallel helical tubes under convective heating condition. Ann Nucl Energy. 2024;201(2):110418. doi:10.1016/j.anucene.2024.110418.
17. Lu X, Wu Y, Zhou L, Tian W, Su G, Qiu S, et al. Theoretical investigations on two-phase flow instability in parallel channels under axial non-uniform heating. Ann Nucl Energy. 2014;63:75–82. doi:10.1016/j.anucene.2013.07.030.
18. Wang S, Yang BW, Mao H, Lin YC, Wang G. The influence of non-uniform heating on two-phase flow instability in subchannel. Nucl Eng Des. 2019;345(3):7–14. doi:10.1016/j.nucengdes.2019.01.024.
19. Ding XY, Chen ZQ, Wen QL, Ruan SH, Qiao PR. Numerical investigation on thermal hydraulics of helical coil tube once through steam generator for LBE fast reactor. Nucl Power Eng. 2021;42(4):21–6. (In Chinese). doi:10.13832/j.jnpe.2021.04.0021.
20. Yang Y, Li Y, Wang C, Wang T, Lan Z, Zhang D, et al. Parametric sensitivity analysis of liquid metal helical coil once-through tube steam generator. Nucl Eng Des. 2021;383(12):111427. doi:10.1016/j.nucengdes.2021.111427.
21. Liu J, Li H, Liu S, Tian Y, Tang L. Steady and transient analysis on thermal hydraulic characteristic of helical coiled once-through steam generator of liquid metal fast reactor. Ann Nucl Energy. 2025;210:110877. doi:10.1016/j.anucene.2024.110877.
22. Itō H. Friction factors for turbulent flow in curved pipes. J Basic Eng. 1959;81(2):123–32. doi:10.1115/1.4008390.
23. Santini L, Cioncolini A, Lombardi C, Ricotti M. Two-phase pressure drops in a helically coiled steam generator. Int J Heat Mass Transf. 2008;51(19–20):4926–39. doi:10.1016/j.ijheatmasstransfer.2008.02.034.
24. Wang M, Zheng M, Yan J, Lin S, Xiao Y. Experimental and numerical studies on two-phase flow instability behavior of a parallel helically coiled system. Ann Nucl Energy. 2020;144(6):107588. doi:10.1016/j.anucene.2020.107588.
25. Papini D, Colombo M, Cammi A, Ricotti ME. Experimental and theoretical studies on density wave instabilities in helically coiled tubes. Int J Heat Mass Transf. 2014;68(1):343–56. doi:10.1016/j.ijheatmasstransfer.2013.09.035.
26. Zhou Y, Yan X, Wang Y, Liu Y, Huang Y. Experimental study of two phase flow instability in parallel narrow rectangular channels. Ann Nucl Energy. 2012;50(2):103–10. doi:10.1016/j.anucene.2012.07.001.
27. Kakac S, Bon B. A review of two-phase flow dynamic instabilities in tube boiling systems. Int J Heat Mass Transf. 2008;51(3–4):399–433. doi:10.1016/j.ijheatmasstransfer.2007.09.026.